Supporting Information

A dihydroquinoline-conjugated polymer cathode with hieratical structure and abundant redox-active sites for aluminum-ion batteries

Zirui Li[a], Mingyue Kang[a], Chuanyi Li[a], Tianliang Tan[a], Zhicheng Wu[a], Hongyu Fan[b], Xuejing Shen[a], Tao Sun[a]* Zhanjun Wu[a,c]*

[a] School of Fiber Engineering and Equipment Technology, Jiangnan University, Wuxi 214122, PR China

[b] School of Science, Jiangnan University, Wuxi 214122, PR China

[c] School of Materials Science and Engineering, Dalian University of Technology, Dalian 116024, PR China

*Corresponding author: Tao Sun, Zhanjun Wu

E-mail address: suntao@jiangnan.edu.cn

1. Material and methods

1.1 Materials:

Phenazine, sodium dithionite, sodium tert-butoxide, 2-dicyclohexylphosphino -2',6' -diisopropoxybiphenyl (S-Phos) were provided by Macklin. Chloro-(2-dicyclo hexyl -phosphino-2',6'-diisopropoxy-1,1'-biphenyl)[2-(2'-amino-1,1'-biphenyl)] palladium (II) (Energy Chemical), 2,7-Dibromonaphthalene were purchase from Energy Chemica. $AlCl_3$, (99.99%) and 1-ethyl-3-methylimidazolium chloride (Sigma Aldrich, 97.0%) were supplied by Sigma Aldrich. MWCNTs were purchase from Shenzhen Suiheng Graphene Technology Co., Ltd. Anhydrous ethanol, toluene and methanol were obtained from Sinopharm Chemical Reagent Co., Ltd. Graphene oxide (GO, 1.0

wt.%) was supplied by the Sixth Element (Changzhou) Materials Technology Co., Ltd. PVDF, N-methyl-2-pyrrolidone (NMP) and acetylene black provided by Guangdong Canrd New Energy Technology Co., Ltd. All chemicals were utilized as received without additional purification.

1.2 Synthesis of 5,10-dihydrophenazine

5,10-Dihydrophenazine (DHPNZ) was synthesized via the reduction of phenazine (PNZ) following a reported procedure [1]. Briefly, 2.0 g of PNZ, 50 mL of ethanol, and 23.3 g of $Na_2S_2O_4$ were dissolved in 200 mL of deionized water. The mixture was transferred into a three-neck round-bottom flask pre-purged with argon and stirred under an argon atmosphere at 120 °C for 4 h. After cooling to room temperature, the prepared mixture was filtered, and the resulting solid product was washed thoroughly with deionized water and then dried in a vacuum oven at 70 °C for 24 h to yield a light-green powder (1.75 g, 87.5% yield). The obtained DHPNZ was stored in an argon-filled glovebox for subsequent use.

1.3 Synthesis of NaphPz

In an argon-filled glovebox, 5,10-dihydrophenazine (183 mg, 1.00 mmol), RuPhos ligand (14 mg, 0.03 mmol), 2,7-dibromonaphthalene (287 mg, 1.00 mmol), RuPhos Pd G2 precatalyst (23 mg, 0.03 mmol), and t-BuONa (481 mg, 5.00 mmol) and 50 mL toluene were added to a 150 mL Schlenk flask. Under argon atmosphere, continue stirring until the reactants are completely dissolved. The mixture was then heated to 110 °C and react for 48 h. After cooling to room temperature, the mixture was centrifuged, and the resulting solid was sequentially washed five times with toluene, methanol, and deionized water. The product was collected and dried in a vacuum oven at 70 °C for 24 h, and obtained as a solid product (yield: 285 mg, 92.2%).

1.4 Preparation of multi-walled carbon nanotube and graphene oxide-coated separators (MCNT-GO-S)

95 mg graphene oxide (GO) was ultrasonically dispersed in 200 ml deionized water. The resulting GO suspension was vacuum-filtered onto a GF/F separators. Subsequently, a suspension of multi-walled carbon nanotubes (MWCNTs, 95 mg) in a mixture of ethanol and N-methyl-2-pyrrolidone (NMP) was vacuum-filtered onto the GO-coated separators. The modified separators was then removed, placed flat in a forced-air oven, and dried at 70 °C for 12 h to obtain the MWCNT/GO-modified separator (MCNT-GO-S).

1.5 Cell fabrication and electrochemical tests

Cathodes were prepared by mixing NaphPz, acetylene black, and poly(vinylidene fluoride) (PVDF) in NMP at a mass ratio of 7:2:1. The resulting slurry was uniformly coated onto tantalum foil using a coating knife, with a mass loading of approximately 1.0 mg cm^{-2}. The coated electrodes were dried under vacuum at 90 °C for 12 h to remove residual NMP. Electrochemical measurements were performed using Swagelok-type cells assembled in an argon-filled glovebox. Aluminum foil was used as the anode. A modified separator (MCNT-GO-S) and a piece of glass fiber paper (Whatman A) were placed sequentially between the Al anode and the cathode. The electrolyte consisted of an $AlCl_3$/EMImCl ionic liquid with a molar ratio of $AlCl_3$/EMImCl = 1.3. Cyclic voltammetry (CV) tests were conducted using the Chenhua CHI660E electrochemical workstation. The scan voltage range was set to 0.1-2.3 V, and the electrochemical impedance spectroscopy (EIS) tests of the battery were also performed on the Chenhua electrochemical workstation. The equivalent circuit used for EIS fitting is shown below:

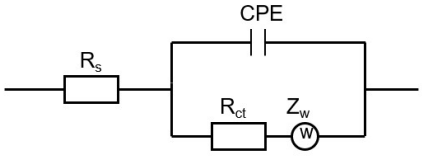

The rate performance and cycling performance of the battery were tested on the

Wuhan Blue Electric CT 4003A.

The testing conditions of the Galvanostatic Intermittent Titration Technique (GITT) are as follows: a constant current density of 100 mA g^{-1} is applied for 10 minutes, followed by a 10 min equilibration period. The D_{Al}^{3+} was calculated using the following equation:

$$D_{Al^{3+}} = \frac{4}{\pi\tau}\left(\frac{m_b V_m}{M_b S}\right)^2 \left(\frac{\Delta E_s}{\Delta E_\tau}\right)^2$$

Among this equation, τ is the relaxation time, mb and Vm are the mass and molar volume, Mb is the molar mass, S is the contact area between the electrolyte and active substance, ΔEs is the change in voltage during the open circuit, ΔEs is the voltage change, and ΔEτ is the current pulse.

All electrochemical tests were conducted at a constant temperature of 26 °C.

1.6 Materials characterizations

Functional group information of the PZ monomer and NaphPz polymer powders was obtained using Fourier transform infrared spectroscopy (FTIR, Thermo Nicolet iS10). Solid-state 13C nuclear magnetic resonance (NMR) spectra were recorded on a Bruker Avance III HD 400 MHz spectrometer. X-ray diffraction (XRD) patterns were collected using a Bruker AXS D2 Phaser A26 diffractometer. Thermogravimetric analysis (TGA) was carried out on a Merrler Toledo TGA/DSC2 thermal analyzer from 30 to 800 °C under a nitrogen atmosphere at a heating rate of 10 °C min^{-1}. The microscopic morphologies of the samples were examined using a scanning electron microscope (SEM, SU8100) and transmission electron microscope (TEM, JEM-2100PLUS). The degree of polymerization of the PZ-based polymers was determined by gas chromatography-time-of-flight mass spectrometry (GC-TOFMS, LECO). Specific surface area and pore size distribution were analyzed using a Microtrac Mrb Belsorp Max fully automatic surface area and pore size analyzer. Elemental composition and distribution were characterized by energy-dispersive X-ray spectroscopy (EDS). X-ray photoelectron spectroscopy (XPS, Thermo Scientific K-

Alpha) was employed to determine the elemental composition and valence state changes of the electrode materials during charge-discharge cycling.

The DFT simulations on the electronic structure of Pz-based polymers and related building blocks was conducted by using Gaussian 09 at the B3LYP level of theory with the 6-31G(d,p) basis set [2].

1.7 Calculation of the theoretical capacity of NaphPz

The theoretical capacity of NaphPz can be calculated according to equation:

$$Q_{NaphPz} = \frac{nF}{3.6M_{NaphPz}}$$

where Q_{NaphPz} is the theoretical specific capacity (mAh g^{-1}), n is the theoretical electron-transfer numbers, F is the Faraday constant (96485 C mol^{-1}) and M_{NaphPz} is the relative molecular weight of one repeating unit (308 g mol^{-1}). Therefore, the theoretical capacity of PPHZ can be determined as follows:

$$Q_{NaphPz} = \frac{3 \times 96485}{3.6 \times 308} \approx 260 \text{ mAh g}^{-1}$$

2. Supporting Figures

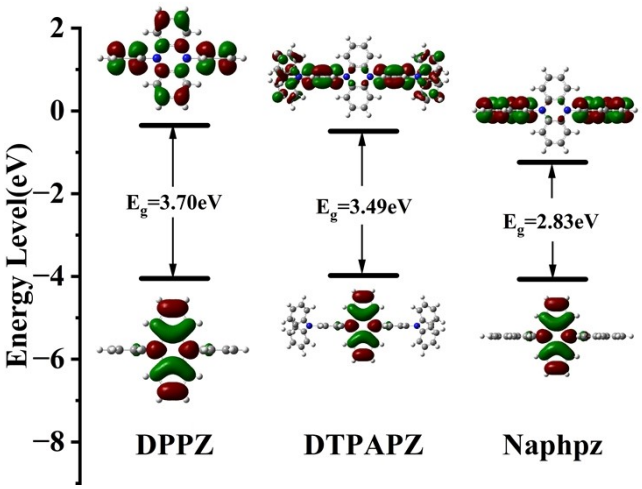

Fig. S1 The band gap of the optimized structures of DPPZ, DTPAPZ, and Naphpz

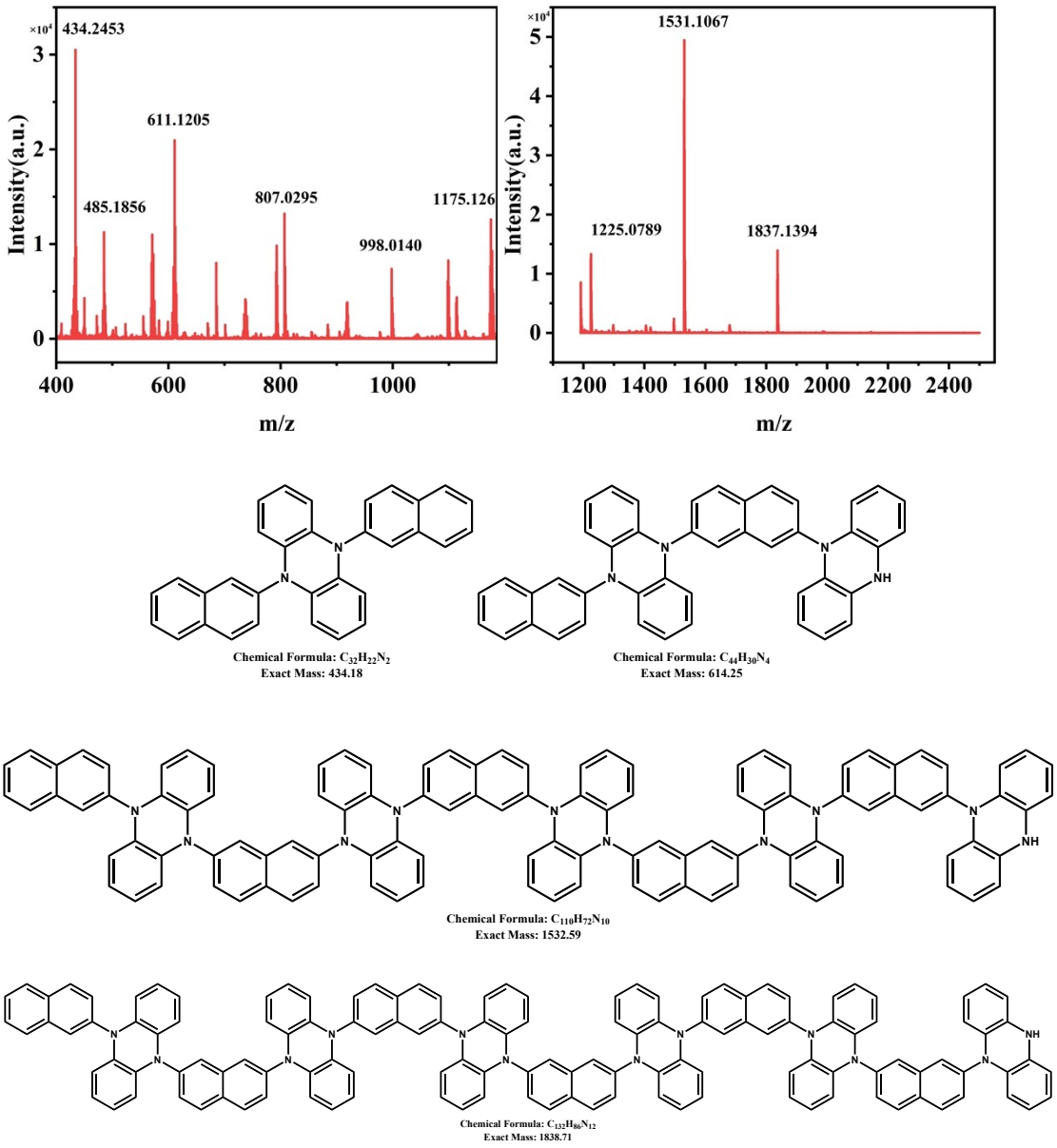

Fig. S2 MALDI-TOF mass spectrum of Naphpz

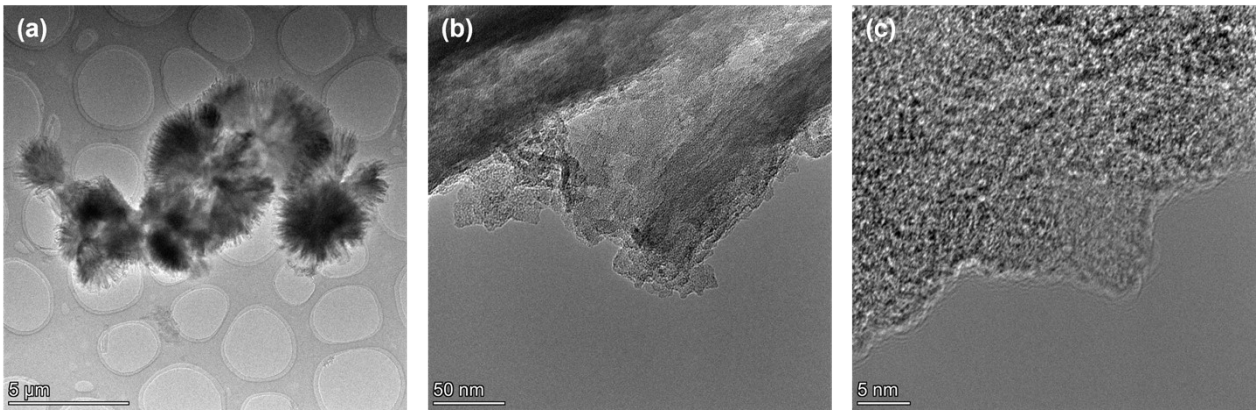

Fig S3 TEM images of NaphPz at different resolutions

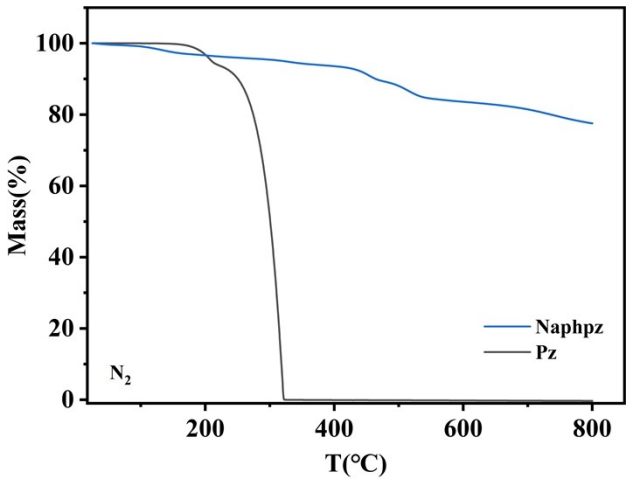

Fig. S4 Thermogravimetric analysis of Naphpz and dihydrophenazine under N_2 atmosphere

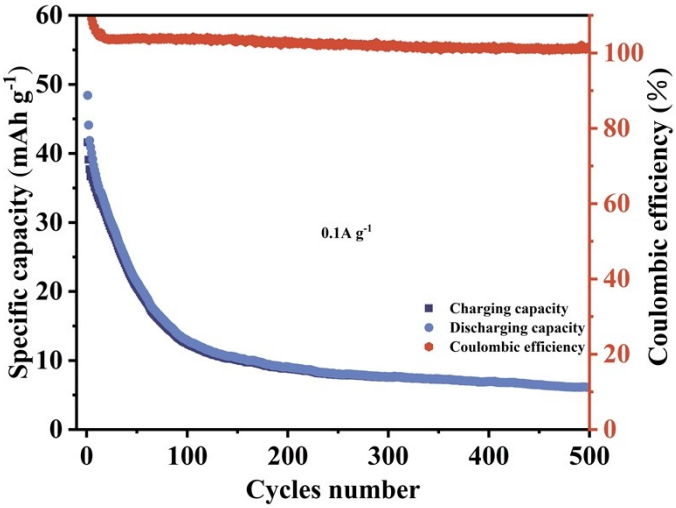

Fi.g S5 Cycling performance and CE of Naphpz cathodes at 0.1 A g^{-1}

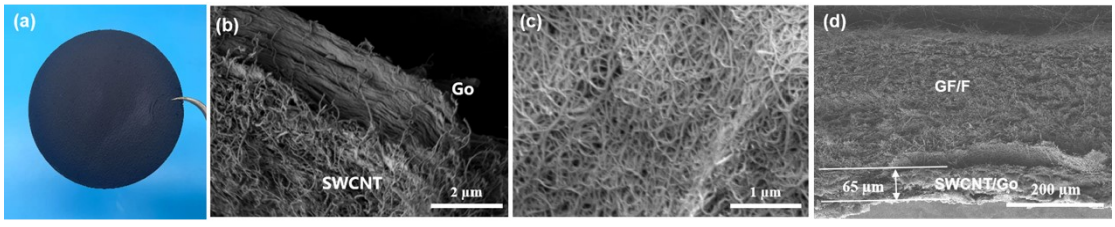

Fig. S6 Photo (a) and SEM images (b), (c) and (d) of MCNT-GO-S

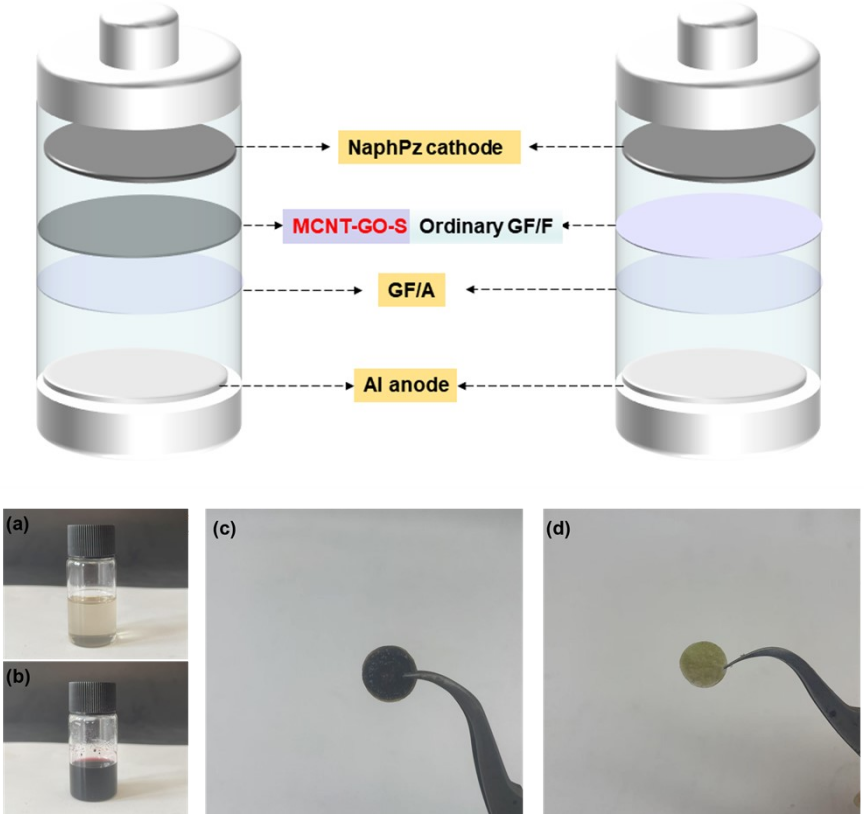

Fig. S7 Photographs of (a) $AlCl_3$/EMImCl ionic liquid (1.3:1 molar ratio), (b) ionic liquid containing NaphPz, and the GF/A separator after 50 cycles in batteries assembled with (c) MCNT-GO-S separator and (d) conventional separator."

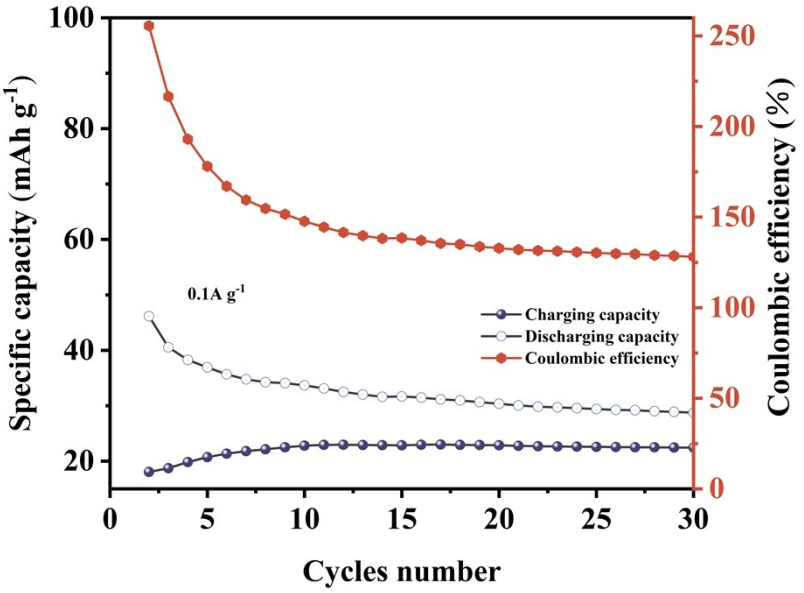

Fig. S8 Cycling performance of MCNT-GO-S separator at 0.1A g^{-1}

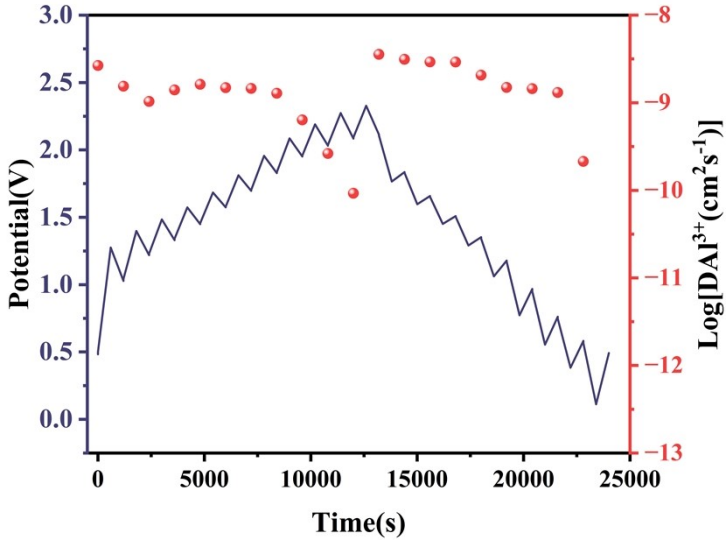

Fig. S9 Discharge-charge GITT profiles of the NaphPz electrode at 0.1 A g^{-1} and corresponding Al^{3+} diffusion coefficients

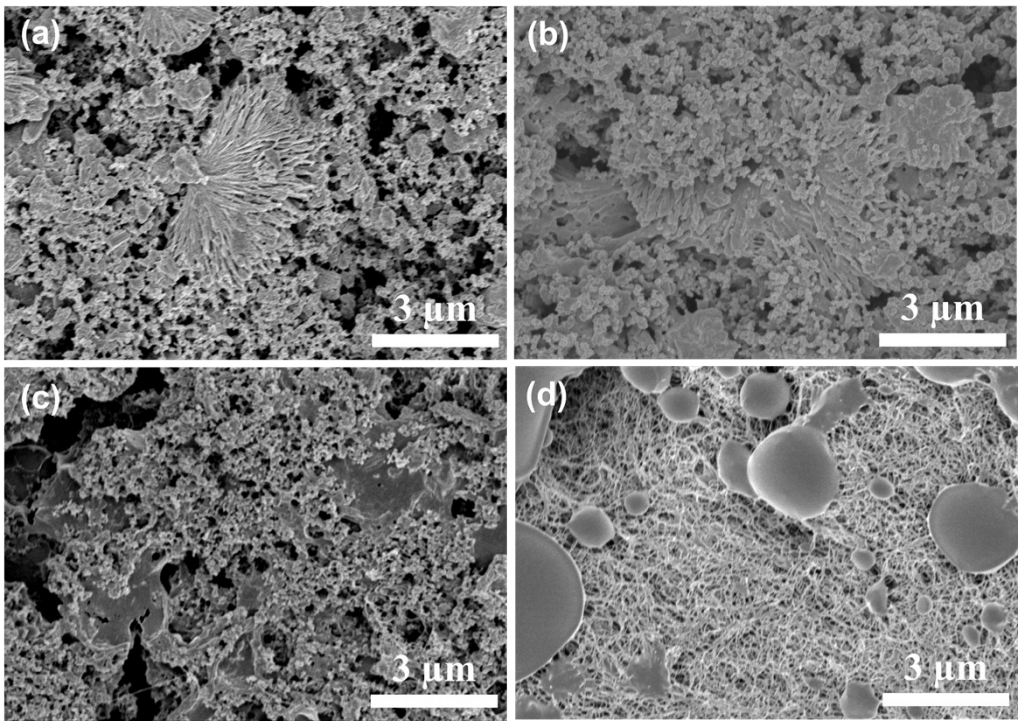

Fig S10 SEM images of initial (a), cycling for12 h (b), and 72 h (c) of Naphpz cathode, and the MCNT-GO-S separator after cycling for 72 h (d).

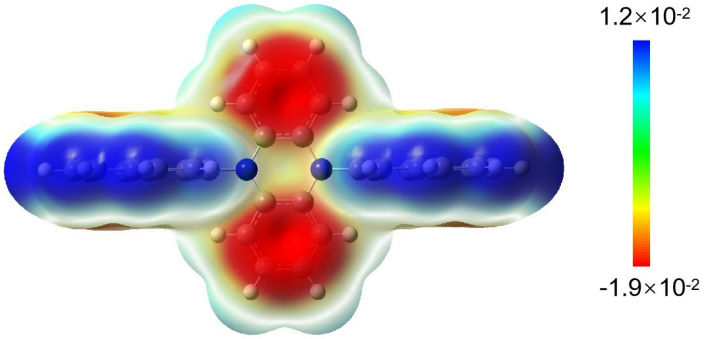

Fig. S11 Molecular surface electrostatic potential (ESP) of Naphpz

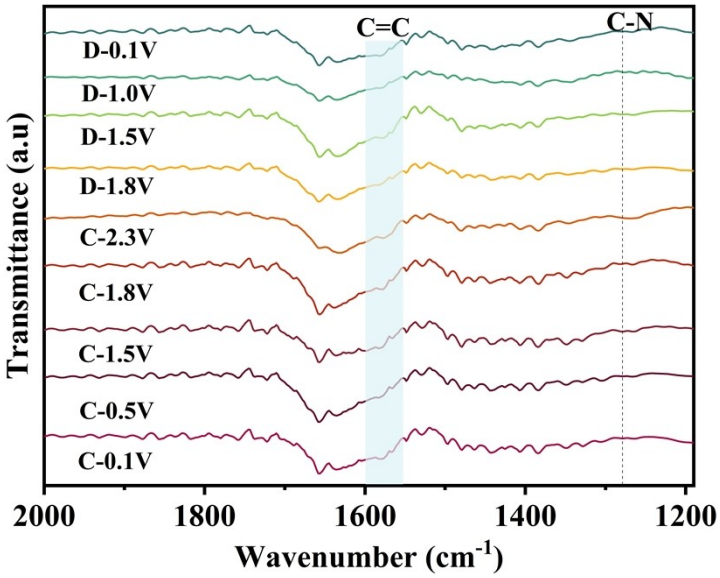

Fig S12 Ex situ FT-IR spectra of Naphpz cathode charging and discharging at different voltages

Table. S2 A comparative assessment of the electrochemical performance of the NaphPz cathode versus previously reported cathode materials in aluminum batteries

Sample	Cycle number	Current density/A g^{-1}	Capacity/mAh g^{-1}	Reference
NaphPz	500	0.8	111	This work
PQ-△	5000	2	53	[3]
PQ-△-HY	500	0.2	114	[3]
Polypyrenes	1000	0.2	100	[4]
2D-COFs	4000	1	82	[5]
BDTO@MXene	500	0.5	134.9	[6]
TPB	250	0.1	175	[7]
TDK	300	0.1	170	[8]
PYTQ-CNT	4000	1	85	[9]
H_2TPP	5000	0.2	75	[10]
Anthracene	800	0.1	130	[11]
TCNQ	500	2	115	[12]
N4	4000	1	116	[13]
TCQ	1000	0.1	56	[14]
Anthraquinone	200	0.1	192.5	[15]

HEPBA	10000	5	79.2	[16]
VO_2–B	1000	1	72.9	[17]
ALMO	1000	1	138	[18]
$(Ti_{0.95}\square_{0.05}O_{1.79}Cl_{0.08}(OH)_{0.13}$	110	3	78.3	[19]

References

[1] J.C. Theriot, C.H. Lim, H. Yang, M.D. Ryan, C.B. Musgrave and G.M. Miyake, *Science*, 2016, **352**, 1082–1086.

[2] M.J. Frisch, G.W. Trucks, H.B. Schlegel, G.E. Scuseria, M.A. Robb, J.R. Cheeseman, G. Scalmani, V. Barone, B. Mennucci, G.A. Petersson, Gaussian 09; Gaussian, Inc.: Wallingford, CT, 2009.

[3] D.J. Kim, D.J. Yoo, M.T. Otley, A. Prokofjevs, C. Pezzato, M. Owczarek, S. J. Lee, J.W. Choi, J.F. Stoddart, *Nat Energy*, 2019, **4**, 51–59.

[4] Y. Liu, Y. Lu, A. Hossain Khan, G. Wang, Y. Wang, A. Morag, Z. Wang, G. Chen, S. Huang, N. Chandrasekhar, D. Sabaghi, D. Li, P. Zhang, D. Ma, E. Brunner, M. Yu and X. Feng, *Angew Chem Int Ed*, 2023, **62**, e202306091.

[5] R. Zhuang, Z. Huang, S. Wang, J. Qiao, J.C. Wu and J. Yang, *Chem. Eng. J.*, 2021, **409**, 128235.

[6] G. Wu, C. Lv, W. Lv, X. Li, W. Zhang and Z. Li, *J. Energy Chem*, 2022, **74**, 174–183.

[7] Y.T. Kao, S. B. Patil, C.Y. An, S.K. Huang, J.C. Lin, T.S. Lee, Y.C. Lee, H.L. Chou, C.W. Chen, Y. J. Chang, Y.H. Lai and D.Y. Wang, *ACS Appl. Mater. Interfaces*, 2020, **12**, 25853–25860.

[8] D.J. Yoo, M. Heeney, F. Glöcklhofer and J.W. Choi, *Nat Commun*, 2021, **12**, 2386.

[9] X. Peng, Y. Xie, A. Baktash, J. Tang, T. Lin, X. Huang, Y. Hu, Z. Jia, D.J. Searles, Y. Yamauchi, L. Wang and B. Luo, *Angew Chem Int Ed*, 2022, **61**, e202206432.

[10] X. Han, S. Li, W.L. Song, N. Chen, H. Chen, S. Huang, S. Jiao, *Adv. Energy Mater*, 2021, **11**, 2101446.

[11] D. Kong, T. Cai, H. Fan, H. Hu, X. Wang, Y. Cui, D. Wang, Y. Wang, H. Hu, M. Wu, Q. Xue, Z. Yan, X. Li, L. Zhao and W. Xing, *Angew Chem Int Ed*, 2022, **61**, e202114681.

[12] F. Guo, Z. Huang, M. Wang, W.-L. Song, A. Lv, X. Han, J. Tu and S. Jiao, *Energy Storage Mater*, 2020, **33**, 250–257.

[13] G. Wang, E. Dmitrieva, B. Kohn, U. Scheler, Y. Liu, V. Tkachova, L. Yang, Y. Fu, J. Ma, P. Zhang, F. Wang, J. Ge and X. Feng, *Angew Chem Int Ed*, 2022, **61**, e202116194.

[14] J. He, X. Shi, C. Wang, H. Zhang, X. Liu, Z. Yang and X. Lu, *Chem. Commun*., 2021, **57**, 6931–6934.

[15] J. Bitenc, N. Lindahl, A. Vizintin, M.E. Abdelhamid, R. Dominko and P. Johansson, *Energy Storage Materials,* 2020, **24**, 379–383.

[16] K. Du, Y Liu, Y Zhao, H. Li, H. Liu, C. Sun, M. Han, T. Ma and Y. Hu. *Adv Mater*, 2024, 36, 2404172.

17] Y. Cai, S. Kumar, R. Chua, V. Verma, D. Yuan, Z. Kou, H. Ren, H. Arora and M. Srinivasan, *J. Mater. Chem. A*, 2020,8,12716-12722.

[18] R. Li, C. Xu, X. Wu, J. Zhang, X. Yuan, F. Wang, Q. Yao, M. Sadesg (Jie Tang) Balogun, Z. Lu and J. Deng, *Energy Storage Materials*, 2022, 53, 514-522.

[19] X, Wu, N. Qin, F. Wang, Z. Li, J. Qin, G. Huang, D. Wang, P. Liu, Q. Yao, Z. Lu and J. Deng, *Energy Storage Materials*, 2021, 37, 619-627.